BJP British Journal of Pharmacology

DOI:10.1111/bph.12984
www.brjpharmacol.org

REVIEW

Carbon nanomaterials combined with metal nanoparticles for theranostic applications

Gloria Modugno[1], Cécilia Ménard-Moyon[1], Maurizio Prato[2] and Alberto Bianco[1]

[1]*Institut de Biologie Moléculaire et Cellulaire, Laboratoire d'Immunopathologie et Chimie Thérapeutique, CNRS, Strasbourg, France, and* [2]*Dipartimento di Scienze Chimiche e Farmaceutiche, Università di Trieste, Trieste, Italy*

Correspondence
UPR3572, CNRS, IBMC, 15 Rue René Descartes, Strasbourg 67084, France. E-mail: a.bianco@ibmc-cnrs.unistra.fr

Received
29 July 2014
Revised
24 September 2014
Accepted
8 October 2014

Among targeted delivery systems, platforms with nanosize dimensions, such as carbon nanomaterials (CNMs) and metal nanoparticles (NPs), have shown great potential in biomedical applications. They have received considerable interest in recent years, especially with respect to their potential utilization in the field of cancer diagnosis and therapy. The many functions of nanomaterials provide opportunities to use them as multimodal agents for theranostics, a combination of therapy and diagnosis. Carbon nanotubes and graphene are some of the most widely used CNMs because of their unique structural and physicochemical properties. Their high specific surface area allows for efficient drug loading and the possibility of functionalization with various bioactive molecules. In addition, CNMs are ideal platforms for the attachment of NPs. In the biomedical field, NPs have also shown tremendous potential for use in drug delivery, non-invasive tumour imaging and early detection due to their optical and magnetic properties. NP/CNM hybrids not only combine the unique properties of the NPs and CNMs but they also exhibit new properties arising from interactions between the two entities. In this review, the preparation of CNMs conjugated to different types of metal NPs and their applications in diagnosis, imaging, therapy and theranostics are presented.

Abbreviations

AuNPs, gold nanoparticles; CBCs, circulating bacteria cells; CNMs, carbon nanomaterials; CNTs, carbon nanotubes; CTAB, cetyltrimethylammonium bromide; CTCs, circulating tumour cells; DOX, doxorubicin; FA, folic acid; GNCs, gold nanoclusters; GNTs, golden carbon nanotubes; GO, graphene oxide; HA, hyaluronic acid; ICP MS, inductively coupled plasma mass spectrometry; IP, IL-13-based peptide; NDs, nanodiamonds; NIR, near-infrared; NPs, nanoparticles; NRs, nanorods; MGMS, magnetic graphene-based mesoporous silica; MIONPs, magnetic iron oxide nanoparticles; MWCNTs, multi-walled carbon nanotubes; PAA, polyacrylic acid; PAT, photoacoustic tomography; PDDA, poly(diallyldimethylammonium chloride); PDT, photodynamic therapy; PE, polyelectrolyte; PEI, polyethyleneimine; PEG, poly(ethyleneglycol); PLA, poly(lactic acid); PLGA, poly(lactic-glycolic acid); PSS, poly-(sodium 4-styrenesulfonate); PTT, photothermal therapy; QDs, quantum dots; rGO, reduced graphene oxide; ROS, reactive oxygen species; SERS, surface-enhanced Raman scattering; SPIONPs, superparamagnetic iron oxide nanoparticles; SPR, surface plasmon resonance; SWCNTs, single-walled carbon nanotubes; SWNHs, single-walled carbon nanohorns; UCL, upconversion luminescence; UCNPs, upconversion nanoparticles; ZnPc, zinc phthalocyanine

Tables of Links

TARGETS
Enzymes
Caspase-3
Urokinase plasminogen activator

LIGANDS	
Cadmium	IL-13
Doxorubicin	Insulin
Folic acid	Paclitaxel
Hyaluronic acid	

These Tables list key protein targets and ligands in this article which are hyperlinked to corresponding entries in http://www.guidetopharmacology.org, the common portal for data from the IUPHAR/BPS Guide to PHARMACOLOGY (Pawson *et al.*, 2014) and are permanently archived in the Concise Guide to PHARMACOLOGY 2013/14 (Alexander *et al.*, 2013).

Introduction

Cancer is a complex disease that arises from DNA mutations and affects cell growth and cell cycle processes. Current treatments for cancer include surgery, radiotherapy, chemotherapy, hyperthermia, immunotherapy, hormone therapy, stem cell therapy and combinations of these modalities. In particular, chemotherapy is used in the treatment of many cancers, but it also presents important limitations such as a lack of specificity, resulting in low concentrations of chemotherapeutic drugs at the tumour sites, along with toxic side effects (Madani *et al.*, 2011).

In this context, many efforts to develop site-directed drug delivery strategies for cancer therapy have been developed. In particular, targeted delivery systems can concentrate more drug molecules at the site of action and optimize the therapeutic response while minimizing undesired toxicity. Some examples include liposomes, micelles, microspheres, natural and synthetic polymer nanoparticles (NPs), metal NPs and carbon nanomaterials (CNMs) (Sajja *et al.*, 2009). Among them, delivery platforms with nanosize dimensions, such as NPs and CNMs, have received considerable interest for their potential utilization in the field of cancer diagnosis and treatment [e.g. bioimaging, drug delivery, photothermal and photodynamic therapy (PDT)]. In fact, nanosize systems have distinct advantages in cancer therapy, starting with their inherent ability to accumulate at tumour sites, much more than in normal tissues, due to the enhanced permeability and retention (EPR) effect of tumours. Blood vessels irrigating tumour tissues have larger pore sizes compared with those in healthy tissue, resulting in preferential tumour accumulation of nanosize anticancer drugs, increased treatment efficacy and reduced systemic toxicity (Fernandez-Fernandez *et al.*, 2011; Shibu *et al.*, 2013).

More importantly, the many functions of nanomaterials provide opportunities to use them as multimodal agents for theranostics, a combination of therapy and diagnosis. Hence, nanomaterials can be used as a single platform to detect tumours, treat them, monitor the treatment response and guide the therapeutic effects. Furthermore, nanoplatforms can be designed to target specific cells by the addition of surface ligands that recognize specific receptors (Janib *et al.*, 2010).

CNMs have attracted particular interest in biomedicine, mainly due to their distinctive physical and chemical properties. CNMs include single-walled carbon nanotubes (SWCNTs), multi-walled carbon nanotubes (MWCNTs), single-walled carbon nanohorns (SWNHs; similar to SWCNTs but closed by a cone at one extremity), graphene, fullerene and nanodiamonds (NDs) (Figure 1) (Liu and Liang, 2012). CNTs and graphene are the most widely used CNMs because of their high surface-area-to-weight ratio and physical and chemical stability. In particular, the former characteristic allows efficient drug loading and bioconjugation (Battigelli *et al.*, 2013). Moreover, CNTs are hollow structures; hence, the inside space can be utilized to encapsulate molecules or NPs. These nanocarbons can readily penetrate into cells and be used as carriers (Lacerda *et al.*, 2012). They also have interesting inherent optical properties, such as fluorescence and Raman scattering, making them useful for optical imaging and sensing applications. They have been used as contrast agents for echography, photoacoustic tomography (PAT), photothermal and Raman imaging (Delogu *et al.*, 2012; Gong *et al.*, 2013). Moreover, their strong optical absorbance in the near-infrared (NIR) region is useful for photothermal ablation of tumours (Kam *et al.*, 2005; Kostarelos *et al.*, 2009; Singh and Torti, 2013).

The attachment of different types of NPs on CNMs has recently attracted great interest (Madani *et al.*, 2013). NPs are also highly promising in non-invasive tumour imaging, early detection and drug delivery, while exhibiting optical and magnetic properties.

In particular, NP/CNM hybrids present advanced and enhanced properties arising from the interactions of metal NPs with CNMs (Guerra and Herrero, 2010; Li *et al.*, 2011; Villalonga *et al.*, 2011). Because CNTs and graphene have a large surface area, they are ideal platforms for the immobilization of NPs. Different strategies have been developed to prepare NP/CNT conjugates: (i) covalent bonding; (ii) electrostatic interactions; (iii) π-stacking; and (iv) hydrophobic interactions. There are many examples of coating of the CNM surface by electrochemical deposition or conjugation chemistry. In particular, polymers have been used as coating agents for CNMs and several coupling strategies adopted for their functionalization, allowing conjugation of NPs to CNMs for biomedical applications (Harrison and Atala, 2007). Alternatively, NPs can also be encapsulated inside the internal cavity of CNTs. However, there are few examples of nanotube filling reported in the literature, mainly due to the difficulty of preparation. Recently, many studies increasingly focus on

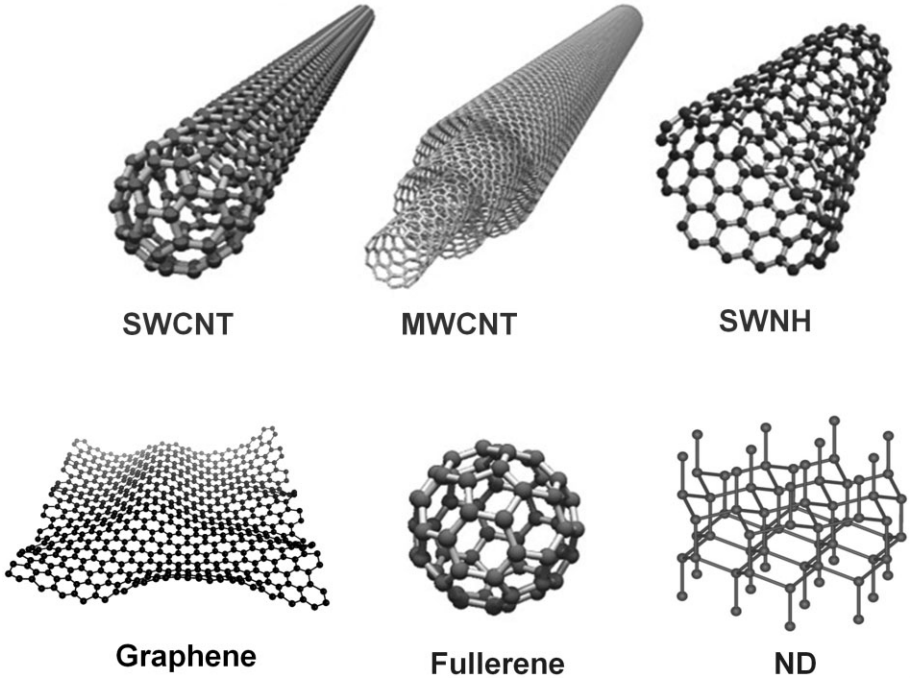

Figure 1
Schematic representation of different CNMs.

functionalization or coating of CNMs with different types of NPs in order to obtain versatile systems with more efficiency for biomedical imaging and cancer therapy.

In this review, we describe the association of CNMs, mainly CNTs and graphene, and NPs for theranostic applications. The article is divided in three parts. More emphasis is given to the most studied systems in this field: CNMs conjugated to (i) iron oxide and (ii) gold NPs, described in the first and in the second section respectively. Thus, recent progress in the preparation of this kind of nanomaterials and their applications in diagnosis, imaging, therapy and theranostics are reported in detail. The third section is dedicated to the conjugation of CNMs with other types of NPs.

Coating of CNMs with iron oxide NPs

Many studies have been reported in the literature on the combination of CNMs and magnetic iron oxide NPs (MIONPs) to generate novel versatile systems that can be employed in biomedicine. Because of their very high transverse relaxivity (i.e. r_2 ~ 141 $mM^{-1}{\cdot}s^{-1}$) and low toxicity, functionalized iron oxide NPs are widely developed as negative (T_2) contrast agents for MRI, for therapy with magnetically induced hyperthermia and for cell labelling. In particular, MIONPs covered by coating agents (e.g. dextran, silicon, PEGylated starch) have been approved, as MR contrast agents, for different clinical applications, for example, for the detection of liver lesions (Laurent *et al.*, 2008).

In this context, the combination of MIONPs with nanomaterials, such as CNTs or graphene, allows for effective MRI contrast enhancement to be achieved, while combining multiple functionalities for therapy. There are only a few studies reporting the filling of CNTs with iron oxide NPs, whereas most studies describe the coating of the nanotube and graphene surface with MNPs. For instance, CNMs have been coated with iron oxide NPs via *in situ* generation of the magnetic NPs by solvothermal synthesis (Shen *et al.*, 2010; Xue *et al.*, 2011). However, this method requires rigorous conditions and the control of particle size is relatively difficult. Alternatively, different strategies have been developed for the coating of CNMs with pre-formed iron oxide NPs based on non-covalent interactions (Mehdipoor *et al.*, 2011) (i.e. electrostatic self-assembly, π-stacking) (Georgakilas *et al.*, 2005; Li *et al.*, 2006; Liu *et al.*, 2009) and sol-gel processes (Narayanan *et al.*, 2009; Kim *et al.*, 2010). Other approaches involve covalent grafting of suitably functionalized MNPs onto oxidized CNTs or graphene by amidation (Xu *et al.*, 2008; Zhou *et al.*, 2010). The strong complexes formed between the carboxylate anions and the iron salts, followed by the precipitation of Fe_3O_4-NPs onto the CNM, have also been exploited as an alternative synthesis method (Masotti and Caporali, 2013).

Diagnosis and imaging. MIONP/CNM hybrids were shown to enhance the detection of cancer cells during MRI, allowing strong MRI contrast both *in vitro* and *in vivo* (Liu *et al.*, 2014b). For example, magnetic $CoFe_2O_4$ NP/MWCNT and Fe_3O_4 NP/MWCNT conjugates exhibited excellent hydrophilicity, low cytotoxicity, neglectable haemolytic activity and a significant MRI negative contrast enhancement effect on cancer cells *in vitro* (Yin *et al.*, 2012). However, *in vivo* MRI studies showed that, after i.v. administration, the T_2-weighted MRI signal in the liver and spleen of mice decreased significantly (Wu *et al.*, 2011).

Khandare *et al*. (2012) prepared a highly versatile multicomponent nanosystem by covalently covering the surface of MWCNTs with Fe_3O_4-NPs, poly(ethyleneglycol) (PEG) and FITC. The CNTs were endowed with magnetic and fluorescent properties and were dispersible in water (Table 1). *In vitro* kinetic experiments demonstrated a rapid (2 h) sustained and time-dependent uptake of the multicomponent system localized at the perinuclear region of MCF7 cancer cells, without toxic effects. The high uptake of the magnetic hybrid makes this fluorescent multicomponent nanosystem an ideal candidate for bioimaging.

Yin *et al*. (2012) have covered MWCNTs with MIONPs and then coated them with multilayer polyelectrolytes (PE). Moreover, folic acid (FA), a targeting agent for tumour cells, was covalently linked to PE. *In vitro* studies on human cervical cancer HeLa cells demonstrated that the FA-PE/MIONP/MWCNTs can be used as a potential targeted imaging contrast agent, with the capacity to obtain strong MRI contrast.

In another study, poly(diallyldimethylammonium chloride) (PDDA) was coated on the surface of acid-treated MWCNTs by electrostatic interactions (Liu *et al*., 2014b). Superparamagnetic iron oxide NPs (SPIONPs) incorporating lactose-glycine adduct (Lac-Gly) as a targeting agent were subsequently immobilized on the surface of the PDDA/MWCNTs. The multifunctional magnetic MWCNTs showed low cytotoxicity on HEK293 and Huh7 cell lines. The T_2 relaxivity of this hybrid material was enhanced in comparison with the free magnetic NPs due to the capacity of the MWCNTs to carry more NPs as clusters. More importantly, after administration of the hybrids to an *in vivo* liver cancer model in mice, a significant increase in tumour-to-liver contrast ratio (277%) was observed in T_2-weighted MR images.

We have reported the covering of MWCNTs with magnetic MIONPs (Lamanna *et al*., 2013). These hybrids easily entered cells, were moderately toxic and displayed good magnetic properties. They were employed for cell labelling, MRI cell tracking and magnetic manipulations. In particular, human prostatic PC3 tumour cells labelled with the NP/CNT hybrids showed magnetic mobility and were detected at a single cell level through high-resolution MRI.

In another study, aminodextran-coated Fe_3O_4-NPs were conjugated to graphene oxide (GO) via formation of amide bond between amines of dextran and carboxylic acids onto the GO sheets (Chen *et al*., 2011). These Fe_3O_4 NP/GO hybrids exhibited good physiological stability, low cytotoxicity and efficient cellular labelling. Indeed, the nanosystem was internalized efficiently by HeLa cells. Compared with Fe_3O_4-NPs alone, these hybrids showed significantly enhanced cellular MRI, being capable of detecting cells at an iron concentration of 20 $\mu g \cdot mL^{-1}$ with a cell density of 1000 $cells \cdot mL^{-1}$. The authors reported, for the first time, the application of GO covered with Fe_3O_4-NPs as a T_2-weighted contrast agent for efficient cellular MRI.

Therapy. MIONP/CNM hybrids have shown great promise as drug carriers and have also been exploited for targeting cancer cells (Pan *et al*., 2011; Zhang *et al*., 2011; Liu *et al*., 2008; Hong *et al*., 2012). In particular, the interest in using CNMs for efficient loading and controlled release of biomolecules is correlated to the different ways the molecule can be linked to CNMs: (i) hydrogen bonding; (ii) π-stacking; (iii) hydrophobic; and (iv) electrostatic interactions. Specifically, in the case of graphene and GO, both sides of the sheets can be functionalized. In addition, the release of the adsorbed molecules from CNMs can be triggered by external stimuli such as pH, temperature, enzymes and an electrical field. In this context, the attractiveness of the combination of magnetic particles with CNTs and graphene relies on the control of drug release that can be modulated and enhanced by a magnetic field. For example, Yang *et al*. (2009; 2011) conjugated FA to a SPIONP/GO nanohybrid by the covalent linkage with amino groups of the 3-aminopropyl triethoxysilane-modified superparamagnetic Fe_3O_4-GO precursor. Finally, doxorubicin (DOX) was loaded onto the surface of the multifunctionalized GO via π-stacking. Cell uptake studies indicated that the multifunctionalized GO can specifically transport the drug to human breast cancer cells (SK3) (folate positive), showing toxicity to tumour cells after loading DOX. These results make it possible to use GO as a multifunctionalized drug carrier for tumour therapy.

Moreover, Turcheniuk *et al*. (2014) prepared magnetic NP/GO hybrids, based on the *ex situ* synthesis of NPs chemically stabilized with 2-nitrodopamine, followed by adsorption onto GO via π–π interactions between 2-nitrodopamine and the aromatic rings of GO. Then, insulin was adsorbed onto GO, showing a pH-dependent loading, with high stability at acidic pH, and insulin release in basic conditions. Moreover, *in vitro* experiments showed that the insulin adsorbed onto the magnetic NP/GO hybrids was strongly resistant to the acidic pH encountered in the gastric environment. This result opens up new ways for further investigating the potential applications of these hybrids for treatment of patients with insulin deficiency.

Furthermore, Fe_3O_4/CNM complexes have shown promising results for inducing apoptotic cancer cell death using a magnetic-targeted therapy, photothermal therapy (PTT) and PDT thanks to the combination of the magnetic properties of NPs with the optical properties of CNMs. For example, a Fe_3O_4/GO hybrid, endowed with superparamagnetic behaviour, was evaluated for localized hyperthermia treatment of cancer (Bai *et al*., 2012). In particular, the temperature of a physiological suspension containing the Fe_3O_4/GO hybrid and exposed to an alternating current magnetic field increased to more than 90°C. Because the optimum localized temperature seems to be around 43°C for local thermal therapy, this hybrid material looks promising for localized hyperthermia treatment of cancers.

Theranostic applications. On-demand control of NP/CNM hybrids by a magnetic field combined with non-invasive monitoring opens new prospects for targeted therapies and potential biomedical applications in theranostics.

In this context, the anticancer drug DOX was loaded onto $CoFe_2O_4$/MWCNTs (DOX/MIONP/MWCNTs) by π-stacking and subsequently released in a sustained and pH-responsive way (Wu *et al*., 2011). Cobalt ferrite ($CoFe_2O_4$), belonging to the family of spinel-type ferrites, has already been used for biomedical applications, especially for MRI contrast enhancement and hyperthermia. The high magnetic anisotropy and saturation magnetization of cobalt ferrite give rise to suitable magnetic behaviour at room temperature (Tung *et al*., 2003). Importantly, the DOX-loaded $CoFe_2O_4$/MWCNT conjugate

Table 1

Coating of CNMs with iron oxide NPs

Type of CNM	Type of NP	Additional functionalization	*In vitro* models	*In vivo* models	Applications	Reference
MWCNT	Fe_3O_4NP	PEG and FITC	MCF7 human breast cancer cells	/	Fluorescence bioimaging and MRI	Khandare *et al.*, 2012
MWCNT	MIONP	PE and FA	HeLa human cervical cancer cells	/	MRI	Yin *et al.*, 2012
MWCNT	SPIONP	PDDA and Lac-Gly	HEK293 human embryonic kidney cells and Huh7 hepatocellular carcinoma cells	Tumour-bearing mice	MRI	Liu *et al.*, 2014b
MWCNT	MIONP	/	PC3 human prostatic tumour cells	/	MRI	Lamanna *et al.*, 2013
GO	Aminodextran-coated Fe_3O_4NP	/	HeLa cells	/	MRI	Chen *et al.*, 2011
GO	3-Aminopropyl triethoxysilane modified SPIONP	FA and DOX	SK3 human breast cancer cells	/	Chemotherapy	Yang *et al.*, 2009; 2011.
GO	2-Nitrodopamine modified MIONP	Insulin	HEK cells	*Xenopus laevis* oocytes	Insulin release	Turcheniuk *et al.*, 2014
GO	SPIONP	/	/	/	PTT	Bai *et al.*, 2012
MWCNT	$CoFe_3O_4$-NP	DOX	HeLa cells	/	MRI and chemotherapy	Wu *et al.*, 2011
MWCNT	MIONP	FA-PAA; DOX and FITC	U87 cells	/	Fluorescence bioimaging and magnetic chemotherapy	Lu *et al.*, 2012
GO	SPIONP	PEG and DOX	4T1 murine breast cancer cells	4T1-tumour-bearing BALB/c mice	MRI; magnetic chemotherapy and magnetic PTT	Ma *et al.*, 2012
rGO	MIONP	C18PMH–PEG and Cy5	4T1 cells	4T1-tumour-bearing BALB/c mice	Fluorescence bioimaging; MRI; PET and PTT	Yang *et al.*, 2012
GO	SPIONP	Chitosan; DOX and p-DNA	A549 human lung epithelial cells and C42b human prostate cancer cells	Prostate tumour-bearing TRAMP mice	MRI; chemotherapy and gene therapy	Wang *et al.*, 2013a
rGO	MIONP	Mesoporous silica; IP; PEG and DOX	U251 human glioma cells	Glioma-bearing mice	MRI; chemotherapy and PTT	Wang *et al.*, 2014b; 2013c
MWCNT	MIONP	/	Murine renal carcinoma cells and MDA-MB-231 human breast cancer cells	*Nu/nu* mice with murine renal carcinoma fragments	MRI and PTT	Ding *et al.*, 2011

/, no data available.

exhibited notable cytotoxicity to HeLa cells due to the intracellular release of DOX. These results suggested that MIONP/CNTs may be used as both an effective MRI contrast agent and a drug delivery system for simultaneous cancer diagnosis and chemotherapy. Lu *et al*. (2012) prepared a FA-derivatized polyacrylic acid (PAA)/Fe_2O_3 NP/MWCNT complex for loading DOX with the aim of developing a magnetic dual-targeted nanocarrier for drug delivery and chemotherapy (FA-PAA/MIONP/MWCNTs) (Figure 2). This hybrid nanomaterial was also labelled with FITC for cellular imaging. At low pH conditions, typical of the environment encountered in intracellular endosomes, DOX was efficiently released from the internalized nanocarrier in the cytoplasmic region and then entered the nucleus to induce cell death. The IC_{50} of this DOX-loaded hybrid was ~30% of that of free DOX. Moreover, this system could be guided by an external magnetic field. In particular, the magnetic manipulation, in combination with specific ligand–receptor interactions, was investigated for targeted drug delivery. Indeed, *in vitro* experiments suggested that the application of a magnetic field under the cell culture could increase the concentration of the fluorescent magnetic nanocarrier (FITC/FA-PAA/MIONP/MWCNTs), resulting in effective cell killing, without affecting normal (control) cell growth. Furthermore, the hybrid loaded with DOX was more effective at killing cells than the same dose of free DOX, due to the magnetic targeting.

Moreover, in a recent study, a multifunctional system based on SPIONP/GO was covalently functionalized with PEG, leading to high stability in physiological solutions and no cellular toxicity (Ma *et al*., 2012). DOX was loaded onto the hybrid via π-stacking, forming a DOX/PEG-SPIONP/GO complex, which enabled magnetically targeted drug delivery. A magnet was placed under the cell culture dish and confocal fluorescence images were registered after 24 h of incubation with the hybrid to track DOX. After being exposed to NIR laser irradiation for 20 min, the nanohybrid was able to selectively kill 4T1 cells that were localized close to the magnet, without affecting the viability of the cells outside of the magnetic field. Moreover, due to its strong optical absorbance from the visible to the NIR region, the hybrid, guided by the magnetic field, was also utilized for localized photothermal ablation of cancer cells. Finally, for the first time, an MRI of tumour-bearing mice was performed *in vivo* using this PEG-SPIONP/GO hybrid as a T_2 contrast agent.

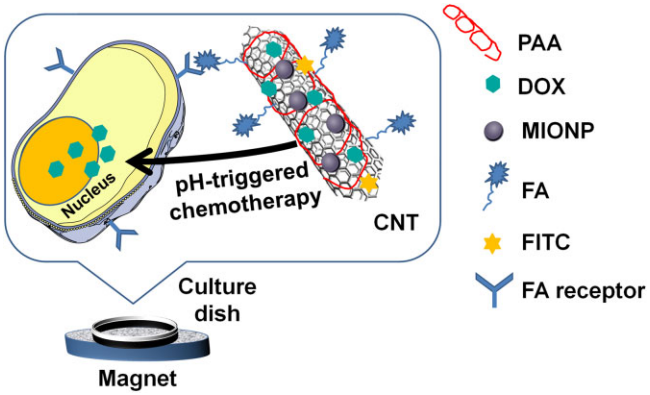

Figure 2

Schematic representation of *in vitro* pH-triggered doxorubicin (DOX) delivery and release using FITC/FA-PAA/MIONP/MWCNT hybrids in the presence of a magnetic field. PAA, polyacrylic acid; MIONP, magnetic iron oxide nanoparticles; FA, folic acid; FITC, fluorescein isothiocyanate.

In contrast, Yang *et al*. (2012) utilized a MIONP/reduced GO (rGO) hybrid non-covalently functionalized with a PEG-grafted poly(maleic anhydride-alt-1-octadecene) (C18PMH-PEG) polymer for multimodal imaging-guided PTT of cancer. Three different imaging techniques of tumour-bearing mice were carried out, revealing high tumour uptake of the conjugate in 4T1 murine breast tumour mice: (i) fluorescence via the use of cyanine 5, which was covalently linked to the amino groups of C18PMH-PEG-NH_2; (ii) MRI; and (iii) PAT, by exploiting the properties of the MIONPs and rGO respectively. In particular, PAT relies on the photoacoustic effect of light absorbers and offers a markedly increased imaging depth compared with traditional optical imaging. PEG/MIONP/rGO with high NIR absorbance appeared to be a strong contrast agent in photoacoustic imaging. This characteristic of the PEG/MIONP/rGO conjugate was also used for *in vivo* MRI-guided PTT, leading to tumour ablation upon irradiation at 808 nm at low power density (0.5 $W{\cdot}cm^{-2}$). This PEG/MIONP/rGO hybrid did not appear to have any obvious toxic effects *in vitro* or side effects *in vivo* at the tested doses.

Recently, a SPIONP-coated GO was covalently functionalized with chitosan at the carboxylic functions, making the hybrid stable, water dispersible and biocompatible, thereby providing an excellent platform for simultaneous targeted cancer chemotherapy, gene therapy and MRI (Wang *et al*., 2013a). In particular, SPIONPs endowed GO with enhanced T_2 contrast. *In vivo* studies and MRI have shown that this nanomaterial accumulates in tumours. Moreover, DOX loaded onto the hybrid was released faster at pH 5.1 than at pH 7.4 and was twice as effective at killing A549 lung cancer cells than free DOX. Finally, the nanomaterial was used to deliver plasmid DNA (p-DNA) encoding GFP (into A549 lung cancer cells and C42b prostate cancer cells). In addition, i.v. administration of p-DNA/DOX/SPIONP/chitosan-GO into tumour-bearing mice showed both GFP expression and DOX accumulation at the tumour site, 24 and 48 h after its administration. This multifunctional nanosystem provides a robust and safe theranostic platform, which integrates targeted delivery of both p-DNA and chemotherapeutic drugs, along with enhanced MRI of tumours.

A magnetic rGO-based mesoporous silica (MGMS) has also been investigated, both *in vitro* and *in vivo*, for MRI visualized-synergistic therapy of glioma, which is the most aggressive brain tumour in humans (Figure 3) (Wang *et al*., 2013c; 2014b). In this study, to improve the biocompatibility of the material and impart targeting capability, MGMS and a glioma-targeting ligand, interleukin(IL)-13-based peptide (IP), were both covalently linked to a bifunctional PEG. The therapeutic and IP-mediated targeting ability of the hybrid was evaluated in glioma cells (U251). The results showed (i) water dispersibility and no toxicity resulting from the biocompatible mesoporous silica and PEG coating; (ii) strong NIR absorbance of rGO (for PTT); (iii) high loading capacity and sustained release of DOX due to the adsorption on the mesoporous silica and the π-stacking interactions with GO

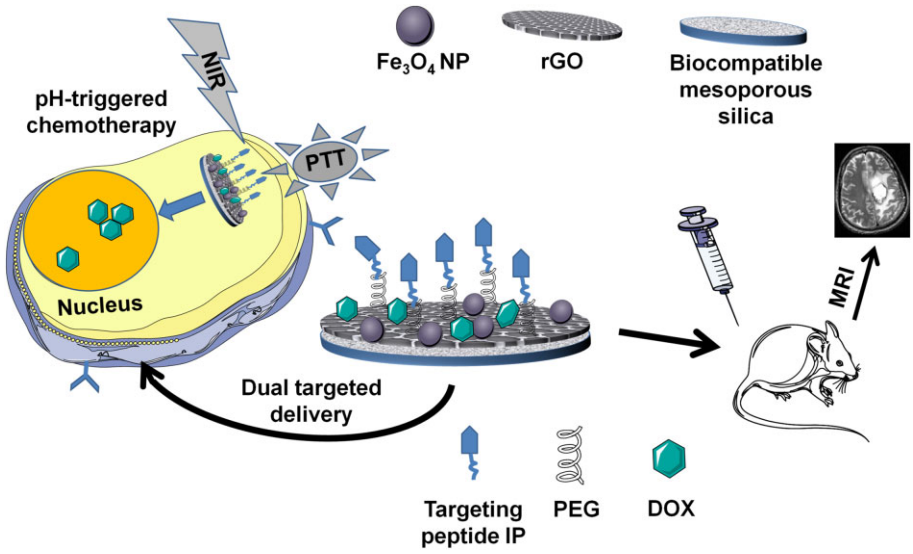

Figure 3

Illustration of the use of multifunctional IP/MGMS hybrids for chemotherapy, PTT and MRI (adapted from Wang *et al.*, 2014b). rGO, reduced graphene oxide, IP, IL-13-based peptide; MGMS, magnetic graphene-based mesoporous silica.

(for chemotherapy); (iv) high transverse relaxivity arising from the Fe_3O_4-NPs (for MRI); (v) high specificity achieved by receptor-mediated targeting and magnetic targeting that induces a strong cellular uptake and cytotoxicity in glioma cells; and (vi) pH- and photothermal-responsive DOX release mediated by changes in the electrostatic and hydrophobic interactions between DOX and the hybrid. The photothermal effect of the hybrid significantly increased the sensitivity of chemotherapy. Moreover, to confirm the IP-mediated targeting function of the hybrid *in vivo* and demonstrate the feasibility of magnetic targeting and MRI, T_2-weighted MR images of differently treated glioma-bearing mice were acquired.

Finally, Ding *et al*. (2011) have demonstrated *in vitro* and *in vivo* that MWCNTs filled with iron NPs are able to serve as a heat transducer for hyperthermia and as an MRI contrast agent. In fact, significant tumour regression was observed in mice treated with magnetic MWCNTs and NIR laser irradiation.

In conclusion, the association of MIONPs with carbon-based nanomaterials is an attractive and promising tool for the development of nanohybrids with potential applications in theranostics.

Coating of CNMs with gold NPs

Gold nanostructures possess unique properties that can be exploited in nanomedicine, for instance as contrast and/or therapeutic agents (Webb and Bardhan, 2014). Gold nanoparticles (AuNPs) exhibit strong absorbance in a wide spectrum, from the visible to NIR regions, due to the surface plasmon resonance (SPR) effect. This property has been exploited for surface-enhanced Raman scattering (SERS)-related applications, such as biomedical imaging and biosensing (Nie and Emory, 1997; Qian *et al.*, 2008a; Qian and Nie, 2008b). SERS allows enhancing Raman signals of molecules adsorbed on noble metal surfaces or NPs by many orders of magnitude. The SPR of AuNPs depends on different parameters, including the size, shape and aggregation state of the NPs, giving possibilities of fine tuning (Boisselier and Astruc, 2009). The extinction coefficient of AuNPs is very high (~1×10^{19} $M^{-1}{\cdot}cm^{-1}$) compared with that of SWCNTs (4.4×10^3 $M^{-1}{\cdot}cm^{-1}$) (Link and El-Sayed, 2000; Schöppler *et al.*, 2011). In the case of graphene derivatives, although rGO displays a sixfold greater NIR absorbance than GO, the low quantum efficiency of rGO and its broad absorption spectrum make it less sensitive to specific wavelengths compared with plasmonic NPs (Robinson *et al.*, 2011; Huschka *et al.*, 2012). The NIR absorption of AuNPs has been exploited for PTT and photoacoustic imaging (Huang *et al.*, 2006; Yavuz *et al.*, 2009; Kim *et al.*, 2011). The development of multimodal PTT agents with enhanced NIR absorbance is required for imaging-guided cancer treatment. In this context, the association of AuNPs and carbon-based nanomaterials allows the design of unique multimodal platforms for disease diagnosis and therapy.

Diagnosis and imaging. CNTs have been used as contrast agents for photoacoustic and photothermal imaging of tumours. Nevertheless, their relatively low NIR absorption restricts *in vivo* applications. To overcome this issue, SWCNTs have been coated with a thin gold layer to enhance the NIR contrast for photoacoustic and photothermal imaging of the lymphatic system (Table 2) (Kim *et al.*, 2009). As CNTs have a relatively low NIR absorption coefficient in comparison with AuNPs, their combination with Au allows very low laser fluence levels, of a few $mJ{\cdot}cm^{-2}$, to be used making it suitable for clinical applications. Additionally, only low concentrations of the so-called golden nanotubes (GNTs) (pico- to femtomolar) are needed, while nanomolar levels are required for conventional agents. The GNTs were conjugated to an antibody in order to target the lymphatic endothelial receptor for *in vivo* mapping of the lymphatic system. The synergy of

Table 2

Coating of CNMs with gold NPs

Type of CNM	Type of NP	Additional functionalization	*In vitro* model	*In vivo* model	Applications	Reference
SWCNT	Au layer	Antibody	/	*Nu/nu* mice	Photoacoustic and photothermal imaging	Kim *et al.*, 2009
SWCNT	Au layer and MIONPs	FA and urokinase plasminogen activator	CTCs	Tumour-bearing mice	Photoacoustic imaging	Galanzha *et al.*, 2009
GO	AuNP	/	HeLa229 cells	/	Raman imaging	Liu *et al.*, 2012
GO	AuNP	/	NE-4C embryonic neuroectodermal stem cells	/	Raman imaging	Kim *et al.*, 2013
SWCNT	AuNP, SPIONP and QD	Silica shell	SKBR3 and MCF7 human breast cancer cells	/	Magnetic field-guided SERS and fluorescence dual-mode imaging	Wang *et al.*, 2014a
SWCNT	AuNP	Thiol-functionalized ionic liquids	HeLa human cervical cancer cells	/	PTT	Meng *et al.*, 2012
SWCNT	AuNP	Sodium alginate and chitosan	HeLa cells	/	PTT	Meng *et al.*, 2014
rGO	AuNS and AuNR	/	HUVECs	/	PTT	Lim *et al.*, 2013
GO	AuNR	PEG	A431 epidermoid carcinoma cells	Mice inoculated with A431 tumour cells	PTT	Dembereldorj *et al.*, 2014
GO	AuNP/AuNR	PEI and p-DNA	HeLa cells	/	Gene therapy	Xu *et al.*, 2013b
GO	AuNR	HA and DOX	Huh-7 hepatocellular carcinoma cells	/	Chemophotothermal therapy	Xu *et al.*, 2013a
MWCNT	AuNP	DOX	A549 human lung epithelial cells	/	Chemotherapy	Minati *et al.*, 2012
GO	AuNP	DOX	HeLa cells	/	Raman imaging and chemotherapy	Ma *et al.*, 2013
rGO	GNC	DOX	HepG2 human liver hepatocellular carcinoma cells	/	NIR fluorescence imaging and chemotherapy	Wang *et al.*, 2011
ND	Au-AgNP	PEG and human transferrin	J5 hepatocellular carcinoma cells	/	PTT	Cheng *et al.*, 2013
SWCNT	AuNP	PEG-FA	KB human carcinoma cells and HeLa cells	/	Raman imaging and PTT	Wang *et al.*, 2012
GO	AuNP	/	HeLa cells and HUVECs cells	White rabbits and tumour-bearing mice	Ultrasound imaging; X-ray CT and PTT	Jin *et al.*, 2013
SWCNT	Au layer	Antibodies specific for *Staphylococcus aureus* protein A	CBCs circulating bacteria cells	*Nu/nu* mice with staphylococcal infection	Photoacoustic diagnosis and PTT of blood infected by bacteria	Galanzha *et al.*, 2012
GO	MIONP and AuNP	PEG-FA	KB cells and 4T1 murine breast cancer cells	Tumour-bearing mice	MRI; X-ray imaging and PTT	Shi *et al.*, 2013

optical (plasmon), thermal, acoustic and bubble overlapping phenomena upon NIR irradiation of individual GNTs shows promise for photoacoustic and photothermal *in vivo* imaging. In another study, the GNTs have been combined with MIONPs for *in vivo* magnetic enrichment and detection of rare circulating tumour cells (CTCs) in blood (Galanzha *et al.*, 2009). The detection of CTCs is of high importance as they are markers for the development of metastasis. The early diagnosis of cancer and prevention of metastasis in humans are still a challenge. The GNTs and magnetic NPs were functionalized with folic acid and with the amino-terminal fragment of the urokinase plasminogen activator in order to target folate receptors and urokinase plasminogen activator receptors respectively. These receptors are overexpressed in many types of cancer cells. A mixture of GNTs and magnetic NPs was administered to tumour-bearing mice and after 20 min a magnet was positioned at the tumour site of the animals. The CTCs targeted by GNTs and the magnetic NPs were captured in the bloodstream of mice and detected by photoacoustic imaging. A two-wavelength system was used to identify the CTCs labelled with both NPs. This strategy based on *in vivo* multiplex targeting, magnetic enrichment, signal amplification and multicolour recognition allowed the concentration of CTCs from a large blood volume in the mice vessels.

Because of its electronic and optical properties, GO has also been used as a Raman probe for cell imaging. However, the weak intensity of the Raman signal currently limits its application. The combination of GO with AuNPs overcomes this problem, as a result of the enhancement of the Raman intensity by SERS (Liu *et al.*, 2012). In this case, the sensitivity for cell imaging was significantly improved and the acquisition times were shorter. AuNP/GO hybrids have also been used for SERS-based biomolecular detection for *in situ* monitoring of stem cell differentiation (Kim *et al.*, 2013).

In addition to AuNPs, CNTs have also been combined with other types of NPs for multimodal imaging. Indeed, because of their high specific surface area, SWCNTs have been used as a building scaffold for the adsorption of SPIONs and AuNPs via electrostatic interactions (Figure 4) (Wang *et al.*, 2014a). This nanohybrid was then coated with a silica shell, onto which fluorescent CdSe/ZnS core-shell QDs were adsorbed. The AuNPs were used as the SERS substrate to link Raman-active molecules. *In vitro* experiments using human breast cancer cells showed that the nanoprobe can be used for magnetic field-guided SERS and fluorescence dual-mode imaging of live cells. This strategy is versatile as different QDs and Raman-active molecules can be used.

Overall, the coating of CNTs and graphene derivatives, mainly GO, is beneficial not only for SERS-based Raman imaging *in vitro* but also for photoacoustic and photothermal imaging *in vivo*, providing attractive opportunities for diagnosis.

Therapy. The enhanced NIR absorption of hybrid conjugates of AuNPs and carbon-based nanomaterials can be exploited for enhanced PTT or combination therapy. For instance, AuNP/CNT hybrids prepared by the growth of AuNPs on SWCNTs coated with thiol-functionalized ionic liquids have been shown to be efficient at inducing hyperthermia of HeLa cells due to their enhanced NIR absorption, resulting in rapid cell death (Meng *et al.*, 2012). Another AuNP/CNT complex was recently designed for efficient PTT of HeLa cells (Meng *et al.*, 2014). In this study, SWCNTs were coated with two oppositely charged polysaccharides (sodium alginate and chitosan) by use of a layer-by-layer self-assembly approach, followed by the growth of AuNPs. The high density and more uniform distribution of active metal-binding groups on the nanotube surface, such as amino and carboxylic groups, facilitated the formation of the AuNPs.

Hybrids composed of Au and graphene derivatives have also been designed for improved PTT. Most hybrids have been prepared by exploiting the two-dimensional morphology of graphene by coating the sheets with AuNPs or *in situ* growth of AuNPs. A novel and original nanohybrid with a three-dimensional spherical morphology has been designed by

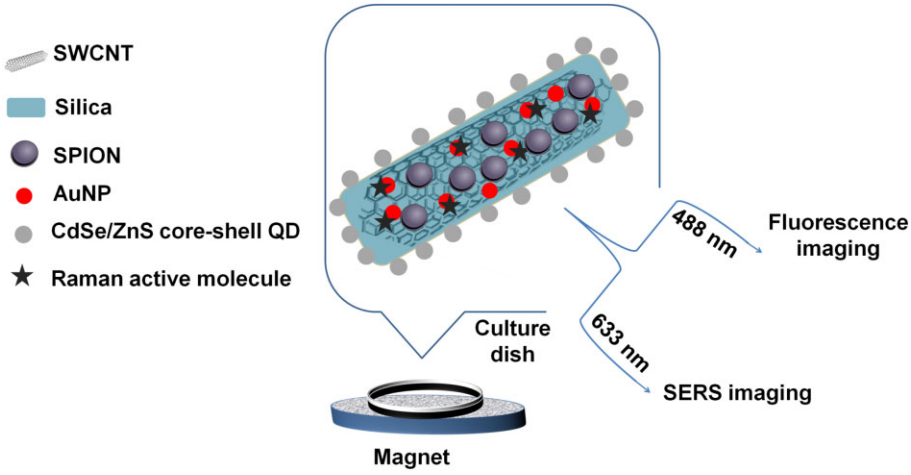

Figure 4

Magnetic field-guided SERS and fluorescence dual-mode imaging of live cells using QD/SPION/AuNP/CNTs (adapted from Wang *et al.*, 2014a). SWCNT, single-walled carbon nanotube; SPION, superparamagnetic iron oxide nanoparticle; AuNP gold nanoparticle; QD, quantum dot.

wrapping rGO sheets onto Au nanoshells (AuNSs) (150 nm in diameter) and Au nanorods (AuNRs) (10 nm width, aspect ratio of 3.5) (Lim *et al.*, 2013). HUVECs were incubated with the AuNS/rGO and AuNR/rGO hybrids. The photothermal effect was enhanced compared with AuNPs coated with GO or non-coated, highlighting the better efficiency of rGO compared to GO due to its higher NIR absorbance. In another study, PEGylated GO coated with AuNRs (long- and short-axis lengths of 39 and 10 nm in average) was also found to be an efficient photothermal agent for elimination of cancer cells (Dembereldorj *et al.*, 2014).

AuNPs and AuNRs coated with GO have been used for gene therapy for the delivery of p-DNA into HeLa cells (Xu *et al.*, 2013b). Polyethyleneimine (PEI) was covalently attached to GO, allowing the condensation of p-DNA via electrostatic interactions with the oxygenated functional groups on GO. PEI/GO has been shown to be efficient at delivering DNA or siRNA into cancer cells (Feng *et al.*, 2011). The encapsulation of AuNPs or AuNRs in GO sheets reduces the cytotoxicity of the NPs and NRs capped with cetyltrimethylammonium bromide (CTAB). This surfactant is widely used in the synthesis of AuNPs, but it is cytotoxic to cells and difficult to remove completely. The *in vitro* transfection efficiency was comparable with PEI and higher than that of PEI/GO, whereas the cytotoxicity was much lower than that of PEI. Thus, the PEI/GO/AuNP and AuNR hybrids may have potential as applications for combined therapy based on gene delivery and PTT.

In another study, the AuNRs encapsulated in GO shells have been employed for *in vitro* targeted chemophotothermal therapy of hepatoma cells (Figure 5) (Xu *et al.*, 2013a). Hyaluronic acid (HA) was covalently attached onto GO to target these cells. Finally, DOX was loaded on the HA/GO/AuNRs. The conjugate was pH-sensitive and NIR light triggered the release of DOX, whereas the photothermal efficiency was higher than that of AuNRs. Overall, the chemophotothermal therapy was synergistic, namely 1.5-fold and fourfold higher than that of separate chemotherapy and PTT respectively.

Theranostic applications. As Au/CNM hybrids have been shown to have improved properties for imaging and therapy, theranostic applications can be envisaged. Indeed, non-spherical AuNPs with nanostar-like shapes were grown on oxidized MWCNTs (Minati *et al.*, 2012). DOX was then adsorbed onto the nanotube sidewall. The broad absorption band of the Au/CNT hybrid in the red and NIR regions allowed cell imaging. After incubation of the DOX/AuNP/CNT conjugate with A549 lung cancer cells, the release of DOX from the nanotube surface and the trafficking of the drug were monitored by laser scanning confocal microscopy. The fluorescence of DOX is quenched when adsorbed onto CNTs and is recovered upon release. After 4 h of incubation, the DOX/AuNP/CNT complex was found inside the cells, according to DOX fluorescence and gold scattering spots. The drug was in close proximity to the Au/CNTs in the cytosol around the nucleus. After 24 h of incubation, DOX was partially released from the nanotube surface and localized in the nucleus, whereas the AuNP/CNTs remained in the perinuclear region.

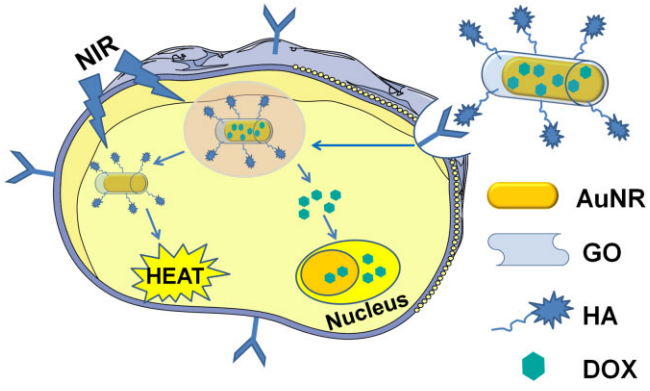

Figure 5
Targeted chemophotothermal therapy using a DOX/HA/GO/AuNRs (adapted from Xu *et al.*, 2013a). AuNr, gold nanorod; GO, graphene oxide; HA, hyaluronic acid.

DOX has also been adsorbed onto AuNPs (less than 100 nm in diameter) wrapped by GO sheets (Ma *et al.*, 2013). The SERS signal from the AuNP/GO hybrid was used for intracellular Raman imaging. By increasing the incubation time, a sustained release of DOX in HeLa cells and a gradual accumulation in the cell nucleus were observed, where the drug can interact with DNA to induce apoptosis. Cell viability was lower after treatment with DOX-loaded AuNP/GO compared with free DOX. Noteworthy, the DOX release was found to be pH-dependent; it was faster and higher at acidic pH. Such pH-triggered drug release is of high interest as the pH in the tumour microenvironment, endosomes and lysosomes is slightly acidic.

Another Au/graphene-based nanohybrid loaded with DOX showed promise as a theranostic application. Indeed, rGO has been coated with gold nanoclusters (GNCs) having an average diameter of 2.5 nm by mixing an aqueous dispersion of rGO with dodecanethiol-CTAB-capped GNCs (Wang *et al.*, 2011). DOX was then adsorbed on the GNC/rGO hybrid via hydrophobic and electrostatic interactions. *In vitro* studies on HepG2 cancer cells showed that free DOX did not distribute well in the cells because nearly half of the drug remained on the cell membrane or between the cells. However, when GNC/rGO was used as a carrier, DOX was well-distributed inside the cells. The release of the drug was monitored by fluorescence imaging. In addition, the NIR fluorescence properties of GNCs were exploited for imaging of the morphology of the cells despite partial fluorescence quenching. The DOX/GNC/rGO conjugate inhibited HepG2 cell growth more strongly than DOX and GNC/rGO alone, while leading to some synergy in inducing karyopyknosis (irreversible condensation of chromatin in the nucleus of necrotic or apoptotic cells). In fact, GNCs cause karyopyknosis of HepG2 cells, but this effect is reduced when GNCs are combined with rGO. Finally, Raman spectroscopy was used to investigate the interactions between DOX/GNC/rGO and HepG2 cells, in particular proteins and DNA. The presence of the hybrid affected protein expression and led to the rupture of DNA chains.

In addition to CNTs and graphene, NDs are another carbon allotrope that has potential for biological applications (Zhang *et al.*, 2009; Li *et al.*, 2010; Smith *et al.*, 2011). In a recent study, NDs have been passivated by conjugating them

with an amino-terminated PEG derivative (Cheng *et al.*, 2013). Thiolation of the amine allowed urchin-like gold/silver bimetallic NPs (5 nm in diameter) to be attached by thiol-metal bonding. The fluorescent NDs display a high photostability without any photobleaching or photoblinking, which is suitable for long-term tracking and labelling. To impart targeting properties, human transferrin was thiolated and then conjugated to Au-AgNP/NDs. *In vitro* studies were conducted on human hepatoma cells overexpressing the transferrin receptor. The cellular uptake over time was monitored using flow cytometry and inductively coupled plasma mass spectrometry (ICP MS) to quantify gold. The amount of transferrin/Au-AgNP/NDs internalized was twice as high as that of the bare Au-AgNP/NDs. Hence, the conjugate bearing transferrin was more efficient for PTT, even when exposed to a less strong laser source.

As SWCNTs display characteristic Raman signals, they have also been used for targeted *in vivo* Raman imaging (Zavaleta *et al.*, 2008). The main advantage of using CNTs as a Raman probe is their high resistance to quenching and photobleaching. Nevertheless, the spectral acquisition times are relatively long. Combining AuNPs with CNTs is one solution that can be used to overcome this problem. In this context, AuNP/SWCNT conjugates coated with PEG have been designed for *in vitro* Raman imaging (Wang *et al.*, 2012). The AuNPs induce a concentration- and excitation–source-dependent SERS effect, showing an enhancement factor of over 20. The AuNP/SWCNTs were also coated with a FA-modified PEG (PEG-FA) chain for Raman imaging of cancer cells using a NIR laser. The acquisition times were shortened compared with SWCNT conjugates not coated with AuNPs. Additionally, a higher PTT-induced cancer cell killing efficacy was observed for the PEG-FA/AuNP/SWCNT conjugate in comparison with PEG/AuNP/SWCNTs and PEG/SWCNTs at the same nanotube concentration. The PTT was highly selective as control experiments on folate receptor-negative cells showed no noticeable cell death after incubation with PEG-FA/AuNP/SWCNTs and laser irradiation.

As an alternative to nanoscale hybrids, microsize carriers have also been designed for theranostic applications *in vivo*. Indeed, microcapsules containing AuNPs and GO were prepared for multimodal imaging and PTT of tumours (Jin *et al.*, 2013). The AuNPs were introduced into poly(lactic acid) (PLA) microcapsules (1.5 μm in diameter) and GO was adsorbed onto the surface via electrostatic layer-by-layer self-assembly. The presence of GO allowed these agents to be used for PTT, whereas the PLA microcapsules and the AuNPs were used as contrast agents to enhance ultrasound imaging and X-ray CT respectively. As AuNPs can attenuate X-rays due to the large atomic number and electron density of gold, they have been used to improve CT imaging. Ultrasonography is useful for real-time imaging, whereas X-ray CT imaging can bring additional anatomical information. *In vivo* ultrasound and X-ray CT imaging were performed in rabbits and mice respectively. A marked improvement in the quality of the ultrasound of the kidney of rabbits was observed a few seconds after i.v. injection of the microcapsules. With regard to X-ray CT imaging, the AuNPs displayed better contrast properties than commercially available iodine-based contrast agents after i.m. injection of the microcapsules in mice. NIR laser-induced PTT of tumour-bearing mice showed that the microcapsules were efficient at destroying tumours (complete within 9 days of treatment), inhibiting tumour growth by as much as 84%. This study presents attractive opportunities as the effectiveness of PTT can be assessed by combining US and CT imaging. Additionally, bimodal imaging could be helpful for guiding PTT by identifying the size and location of the tumour in order to avoid damaging normal tissues.

The GNTs have been investigated for *in vivo* magnetic enrichment, photoacoustic diagnosis and photothermal treatment of blood infected by bacteria (Galanzha *et al.*, 2012). AuNRs and silica-coated magnetic NPs were also explored in this study. The different NPs were conjugated to antibodies specific for *Staphylococcus aureus* protein A and/or lipoprotein absent in mammalian cells. Ultrasensitive detection of circulating bacteria cells (CBCs) was achieved with a threshold sensitivity as low as 0.5 CBCs·mL^{-1}. From the results of this study, an attractive alternative antibacterial treatment was proposed, which is based on the physical destruction of bacteria irrespective of their antibiotic resistance status.

A multifunctional magnetic and plasmonic nanohybrid has been prepared by coating GO with both MIONPs and AuNPs (Figure 6) (Shi *et al.*, 2013). The MIONP/AuNP/GO displayed a strong superparamagnetism and an enhanced optical absorbance in the NIR region. The AuNPs were coated with PEG to enhance the stability of the conjugate in physiological environments and increase its biocompatibility.

Both magnetic and plasmonic properties were exploited for MRI and X-ray imaging *in vivo*. For this purpose, the PEG/MIONP/AuNP/GO was administered intratumorally to tumour-bearing mice. A darkening effect in T2-weighted MR images and a contrast in X-ray images were observed in the tumour. PTT was studied on murine breast cancer 4T1 cells, human carcinoma KB cells and tumour-bearing mice. For *in vitro* studies, the MIONP/AuNP/GO was coated with PEG-FA. The cancer cells were effectively killed upon incubation with PEG-FA/MIONP/AuNP/GO followed by laser irradiation, whereas the cells treated with the MIONP/AuNP/GO coated with PEG were less affected. When folate receptor-negative 4T1 cells were treated in the same conditions, no significant cell damage was noted. The magnetic properties of the nanohybrid were also exploited for targeted PTT. For this purpose, 4T1 cells were incubated with PEG/MIONP/AuNP/GO for 2 h in the presence of a magnetic field placed under the centre of the cell culture dish. After NIR laser irradiation, only the cells near the magnet were killed. Experiments were also conducted *in vivo* in tumour-bearing mice; PEG/MIONP/AuNP/GO was injected intratumorally and PEG/GO was used as the control. NIR irradiation led to the significant destruction of the tumour when the gold conjugate was used, whereas those tumours treated with PEGylated GO were only partially damaged after the PTT treatment.

Overall, we conclude that the association of carbon-based nanomaterials and gold NPs has immense potential for imaging, therapy and theranostic applications.

Coating of CNMs with other types of metal NPs

Other types of NPs, such as QDs (Guo *et al.*, 2008), upconversion NPs (UCNPs) (Wang *et al.*, 2013b), silica (Zhang *et al.*, 2012), SnO_2 (Liu *et al.*, 2013a), Cu_2O (Hou *et al.*, 2013), ZnO

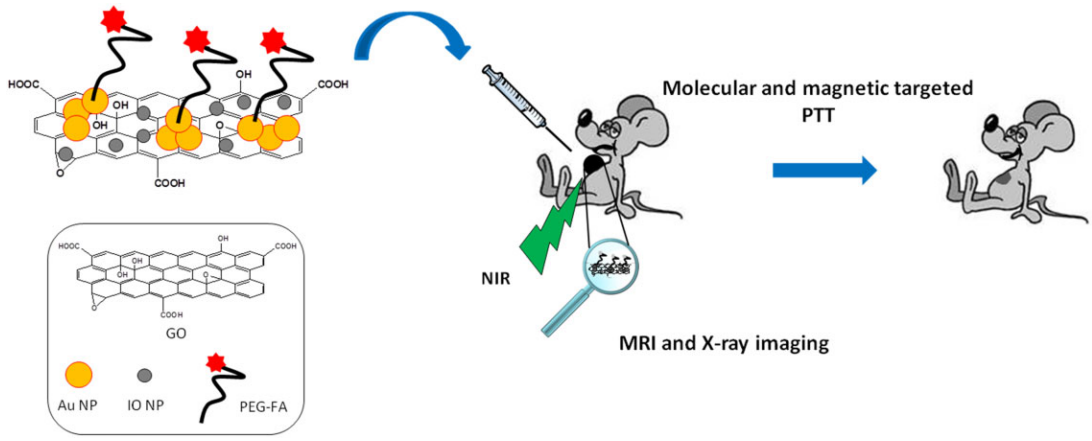

Figure 6
PTT and imaging of tumour-bearing mice using PEG-FA/MIONP/AuNP/GO. MIONP, magnetic iron oxide nanoparticle.

(Chen *et al.*, 2014) and AgNPs (Liu *et al.*, 2013b) have been combined with CNMs (Wildgoose *et al.*, 2006). These NPs themselves have also shown good promise in non-invasive tumour imaging, early detection and drug delivery, while exhibiting optical and magnetic properties that can be exploited for therapy. In this context, the combination of different NPs with CNTs or graphene allows alternative multimodal theranostic hybrid systems to be designed. Generally, NPs have been linked to the CNM surface by either direct attachment or via interactions with a polymer conjugated to either the CNMs or the NPs.

Diagnosis and imaging. For deep tissue tumour imaging, highly intense emissions are required at a frequency close to the NIR range (>800 nm). We have already explained that some CNMs are intrinsically fluorescent in the NIR region, where tissues and biological fluids are practically transparent. However, the emission intensities are quite low and not useful for deep tissue or live animal imaging. In contrast, the optical properties of QDs, which are semiconducting nanocrystals, may be modified based on their size, resulting from quantum confinement effects. In particular, they offer high resistance to photobleaching, thus making them attractive material for biomedical diagnosis applications. Recently, UCNPs, composed of $NaYF_4$, Yb^{3+}, Er^{3+} and Tm^{3+}, have also received considerable interest as fluorescent probes for cancer diagnosis (Liu *et al.*, 2014a). They are characterized by the sequential absorption of two or more photons, leading to the emission of light at a shorter wavelength than the excitation wavelength. They have the significant advantage of possessing a sharp emission bandwidth, long lifetime, adjustable emission, high photostability and low cytotoxicity. More importantly, UCNPs use NIR excitation, thereby significantly enhancing penetration depths and minimizing background autofluorescence, photobleaching as well as photodamage of biological species. Benefiting from such unique advantages, QDs and UCNPs have been successfully employed as promising contrast agents for *in vitro* cell imaging and *in vivo* whole-animal imaging. In particular, the conjugation of CNMs with luminescent NPs, as QDs and UCNPs, offers several advantages for deep tissue imaging, including the possibility of integration with potential drug delivery and cancer therapy systems. Moreover, FA/AgNP/GO hybrids have also been employed for the probing and imaging of cells by monitoring the SERS signals (Table 3) (Liu *et al.*, 2013b). In this case, the inherent Raman signal of GO was significantly enhanced after depositing AgNPs onto its surface.

Therapy. In a recent study, HA adsorbed onto a ZnO NP/rGO hybrid (HA/ZnO NP/rGO) was employed as a multisynergistic platform for targeted cancer therapy (combination of PDT and PTT) (Chen *et al.*, 2014). ZnO NPs are easy to fabricate, inexpensive and exhibit therapeutic effects. Especially, due to their unique phototoxic effect, ZnO has been investigated as attractive reactive oxygen species (ROS) sensitizing agents for anticancer studies. Of particular interest, the photoactivity of ZnO NPs can be significantly enhanced by their combination with graphene, which acts as an excellent electron acceptor to inhibit the quick recombination of the photoexcited electron-hole pairs and thus enhance the generation of ROS. HA has been used as a targeting moiety because of its specific interactions with the CD44 receptor, which is overexpressed in various cancer cells. Indeed, the surface of the ZnO NP/rGO hybrid was coated with multifunctional FITC-labelled HA deoxycholic acid (HA-DA) through hydrophobic interactions between DA and graphene. *In vitro* experiments, performed on MDA-MB-231 cells showed that the ROS generated by ZnO NP/rGO under light illumination (PDT) in combination with the NIR laser-induced hyperthermia (PTT) resulted in a synergistic apoptotic therapy. In fact, PDT or PTT alone only moderately inhibited the growth of MDA-MB-231 cells. In contrast, the combination of PDT and PTT resulted in significant cytotoxicity that was increased in a dose-dependent manner.

Moreover, by a simple and effective chemical precipitation method, GO derivatized with FA was coated with ZnO NPs (Hu *et al.*, 2013). The resulting hybrid combined the photodynamic activity of ZnO and photothermal anticancer effects of GO, with the possibility of direct tumour cell killing using FA as a targeting ligand. Indeed, the conjugation of

Table 3

Coating of CNMs with other types of metal NPs

Type of CNM	Type of NP	Additional functionalization	*In vitro* model	*In vivo* model	Applications	Reference
GO	AgNP	FA	HeLa human cervical cancer cells	/	Raman imaging	Liu *et al.*, 2013b
rGO	ZnO NP	HA-DA and FITC	MDA-MB-231 human breast cancer cells and NIH3T3 mouse embryonic fibroblast cells	/	PDT and PTT	Chen *et al.*, 2014
GO	ZnO NP	FA	HeLa cells	/	PDT	Hu *et al.*, 2013
rGO	Cu_2O nanocrystals	PSS	HK-2 human renal epithelial cells; MDA-MB-231 and A549 human lung epithelial cells	/	PDT and PTT	Hou *et al.*, 2013
MWCNT	QD	PLGA and paclitaxel	PC-3MM2 human prostate carcinoma cells	*Nu/nu* mice	Fluorescence imaging and chemotherapy	Guo *et al.*, 2008
GO	UCNP	PEG and ZnPc	KB human nasopharyngeal epidermal carcinoma cells and HeLa cells	Kunming mice	UCL; PDT and PTT	Wang *et al.*, 2013b

ZnO to FA/GO induced a marked improvement in tumour targeting, as demonstrated by the cellular uptake assay. In addition, this hybrid exhibited significant photodynamic activity, mediated by the generation of ROS under visible light irradiation. Following the generation of ROS, the material caused a reduction in the activity of antioxidant enzymes (superoxide dismutase, catalase and GSH peroxidase) and various apoptotic events in HeLa cells. An increase in the intracellular malondialdehyde level and depolarization of the mitochondrial membrane were also observed. Finally, the FA/ZnO NP/GO hybrid induced apoptotic death by enhancing caspase-3 activity, the main effector caspase involved in apoptosis. In conclusion, this study presents a promising strategy for the use of targeted PDT for cancer treatment.

In addition, a Cu_2O nanocrystal/rGO hybrid decorated with biocompatible poly-(sodium 4-styrenesulfonate) (PSS) exhibited anticancer activity under both visible and NIR light irradiation *in vitro* (Figure 7) (Hou *et al.*, 2013). In contrast to the highly efficient killing of both normal and cancer cells initiated by the photothermal effect, the photocatalytic effect arising from the Cu_2O nanocrystals resulted in the selective killing of cancer cells under visible light irradiation. The photothermal effect on cells was mainly attributed to the protein denaturation in cells initiated by heat. However, this PTT effect was not selective as both cancer and normal cells were killed. It is now well established that semiconductor photocatalysts, such as Cu_2O, can be applied for cancer treatment, due to the production of ROS under excitation by light, which damages several antioxidant mechanisms. Surprisingly, in this work, *in vitro* experiments showed that the degree and rate of ROS production, and oxidation reactions initiated, were dependent on the cell type. In particular, during the first hour of irradiation, normal cells (HK-2) incubated with PSS/Cu_2O NP/rGO hybrid showed nearly 100%

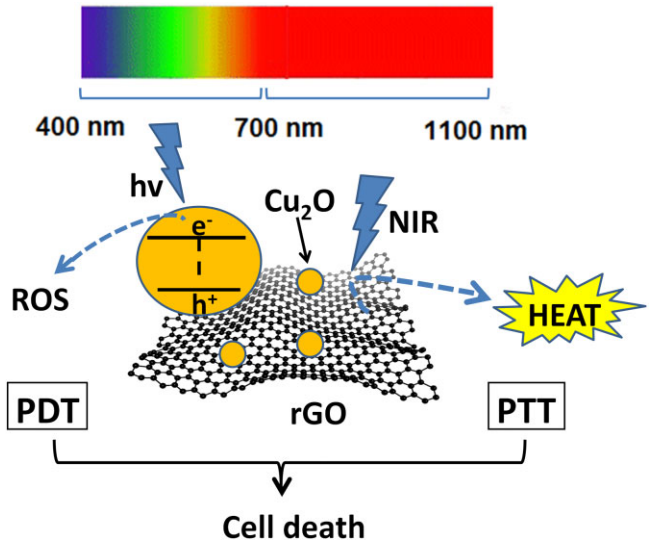

Figure 7

Illustration of PDT and PTT using Cu_2O NP/rGO (adapted from Hou *et al.*, 2013).

viability even at a high hybrid concentration (640 $\mu g \cdot mL^{-1}$), while for cancer cells (MDA-MB-231 and A549) the viability decreased even at a low hybrid concentration of 40 $\mu g \cdot mL^{-1}$. These results demonstrate the selective killing of cancer cells by PSS/Cu_2O NP/rGO under visible light.

Theranostic applications. Recently, a material based on amine-containing QDs conjugated to carboxyl-functionalized MWCNTs was covered by poly(lactic-glycolic

acid) (PLGA) films using a plasma polymerization methodology (Guo *et al*., 2008). With NIR emission around 752 nm, the PLGA/QD/CNTs exhibited a strong luminescence for non-invasive optical *in vivo* imaging. Moreover, the anticancer agent paclitaxel was efficiently loaded onto these PLGA-coated CNTs. The cytotoxicity and antitumour efficacy of this novel drug delivery system was established *in vitro*, using PC-3MM2 human prostate carcinoma cells. Moreover, *in vivo* biodistribution of the PLGA/QD/CNT hybrid was determined using ICP MS by quantifying the mass of cadmium in organs, showing a predominant hybrid uptake in liver, kidney, stomach and intestine.

Wang *et al*. (2013b) reported a multifunctional nanoplatform developed by covalently grafting amino-functionalized core shell-structured UCNPs to GO via a bifunctional PEG. To achieve a multimodal effective therapy, aromatic zinc phthalocyanine (ZnPc) with a high optical absorption coefficient in the phototherapeutic window (600–800 nm) was then loaded onto GO. Cytotoxicity assays demonstrated good biocompatibility and low toxicity of the ZnPc/UCNP/GO hybrid. The nanomaterial was used both *in vitro* and *in vivo* for upconversion luminescence (UCL) imaging probes of cells and whole-body animals with high contrast for diagnosis. Moreover, the hybrid was also explored for PDT and PTT via the generation of cytotoxic singlet oxygen and conversion of laser energy into heat under light excitation. A remarkably improved and synergistic therapeutic effect compared with PTT or PDT alone was obtained, providing high therapeutic efficacy for cancer treatment. Indeed, this multifunctional hybrid shows promise as an integrated theranostic probe for potential UCL image-guided combinatorial PDT/PTT of cancer.

Conclusions

The advent of nanotechnology in biological systems heralds a new chapter in the field of cancer therapy. Particularly, the combination of CNMs with metal NPs, by exerting synergistic effects, is providing novel perspectives for applications in theranostics. Indeed, these systems can easily combine the extraordinary structural, optical, chemical and thermal properties of both CNMs and NPs in a unique nanosystem that can simultaneously detect, image and treat a disease. The results show that the advances made both *in vitro* and *in vivo* are real and of great significance in our understanding of the biological effects of these systems.

Overall, we can conclude that all of the materials described provide a unique opportunity for the preparation of non-invasive *in vivo* theranostic systems that may have a great impact on the development of future therapies against cancer. Nevertheless, the design and preparation of nanomaterials for diagnosis and therapy still present many challenges such as biocompatibility, pharmacokinetics, *in vivo* targeting efficacy and cost-effectiveness. In addition, a full assessment of the risk factors derived from the use of nanomaterials in nanomedicine has to be performed in order to understand their effect on human health and the environment, and to develop specific regulatory guidelines for their clinical applications.

Acknowledgements

This work was supported by CNRS and partly by the ANR Blanc – SIMI 10 – Nanosciences (NANOLUPUS project ANR-12-BS10-012-01). C. M.-M. and A. B. gratefully acknowledge financial support from EU FP7-ICT-2013-FET-F GRAPHENE Flagship project (no. 604391).

Conflict of interest

The authors declare no conflicts of interest.

References

Alexander SPH, Benson HE, Faccenda E, Pawson AJ, Sharman JL, Spedding M *et al*. (2013). The Concise Guide to PHARMACOLOGY 2013/14: Enzymes. Br J Pharmacol 170: 1797–1867.

Bai L-Z, Zhao D-L, Xu Y, Zhang J-M, Gao Y-L, Zhao L-Y *et al*. (2012). Inductive heating property of graphene oxide–Fe_3O_4 nanoparticles hybrid in an AC magnetic field for localized hyperthermia. Mater Lett 68: 399–401.

Battigelli A, Ménard-Moyon C, da Ros T, Prato M, Bianco A (2013). Endowing carbon nanotubes with biological and biomedical properties by chemical modifications. Adv Drug Deliv Rev 65: 1899–1920.

Boisselier E, Astruc D (2009). Gold nanoparticles in nanomedicine: preparations, imaging, diagnostics, therapies and toxicity. Chem Soc Rev 38: 1759–1782.

Chen W, Yi P, Zhang Y, Zhang L, Deng Z, Zhang Z (2011). Composites of aminodextran-coated Fe_3O_4 nanoparticles and graphene oxide for cellular magnetic resonance imaging. ACS Appl Mater Interfaces 3: 4085–4091.

Chen Z, Li Z, Wang J, Ju E, Zhou L, Ren J *et al*. (2014). A multi-synergistic platform for sequential irradiation-activated high-performance apoptotic cancer therapy. Adv Funct Mater 24: 522–529.

Cheng LC, Chen HM, Lai TC, Chan YC, Liu RS, Sung JC *et al*. (2013). Targeting polymeric fluorescent nanodiamond-gold/silver multi-functional nanoparticles as a light-transforming hyperthermia reagent for cancer cells. Nanoscale 5: 3931–3940.

Delogu GL, Vidili G, Venturelli E, Ménard-Moyon C, Zoroddu AM, Pilo G *et al*. (2012). Functionalized multiwalled carbon nanotubes as ultrasound contrast agents. Proc Natl Acad Sci U S A 109: 16612–16617.

Dembereldorj U, Choi SY, Ganbold EO, Song NW, Kim D, Choo J *et al*. (2014). Gold nanorod-assembled PEGylated graphene-oxide nanocomposites for photothermal cancer therapy. Photochem Photobiol 90: 659–666.

Ding X, Singh R, Burke A, Hatcher H, Olson J, Robert A *et al*. (2011). Development of iron-containing multiwalled carbon nanotubes for MR-guided laser-induced thermotherapy. Nanomedicine (Lond) 6: 1341–1352.

Feng L, Zhang S, Liu Z (2011). Graphene based gene transfection. Nanoscale 3: 1252–1257.

Fernandez-Fernandez A, Manchanda R, McGoron AJ (2011). Theranostic applications of nanomaterials in cancer: drug delivery, image-guided therapy and multifunctional platforms. Appl Biochem Biotechnol 165: 1628–1651.

Galanzha EI, Shashkov EV, Kelly T, Kim JW, Yang L, Zharov VP (2009). *In vivo* magnetic enrichment and multiplex photoacoustic detection of circulating tumour cells. Nat Nanotechol 4: 855–860.

Galanzha EI, Shashkov E, Sarimollaoglu M, Beenken KE, Basnakian AG, Shirtliff ME *et al.* (2012). *In vivo* magnetic enrichment, photoacoustic diagnosis, and photothermal purging of infected blood using multifunctional gold and magnetic nanoparticles. PLoS ONE 7: e45557.

Georgakilas V, Tzitzios V, Gournis D, Petridis D (2005). Attachment of magnetic nanoparticles on carbon nanotubes and their soluble derivatives. Chem Mater 17: 1613–1617.

Gong H, Peng R, Liu Z (2013). Carbon nanotubes for biomedical imaging: the recent advances. Adv Drug Deliv Rev 65: 1951–1963.

Guerra J, Herrero MA (2010). Hybrid materials based on Pd nanoparticles on carbon nanostructures for environmentally benign C-C coupling chemistry. Nanoscale 2: 1390–1400.

Guo Y, Shi D, Cho H, Dong Z, Kulkarni A, Pauletti GM *et al.* (2008). *In vivo* imaging and drug storage by quantum-dot-conjugated carbon nanotubes. Adv Funct Mater 18: 2489–2497.

Harrison BS, Atala A (2007). Carbon nanotube applications for tissue engineering. Biomaterials 28: 344–353.

Hong J, Shah NJ, Drake AC, DeMuth PC, Lee JB, Chen J *et al.* (2012). Graphene multilayers as gates for multi-week sequential release of proteins from surfaces. ACS Nano 6: 81–88.

Hou C, Quan H, Duan Y, Zhang Q, Wang H, Li Y (2013). Facile synthesis of water-dispersible Cu_2O nanocrystal-reduced graphene oxide hybrid as a promising cancer therapeutic agent. Nanoscale 5: 1227–1232.

Hu Z, Li J, Li C, Zhao S, Li N, Wang Y *et al.* (2013). Folic acid-conjugated graphene–ZnO nanohybrid for targeting photodynamic therapy under visible light irradiation. J Mater Chem B 1: 5003–5013.

Huang X, El-Sayed IH, Qian W, El-Sayed MA (2006). Cancer cell imaging and photothermal therapy in the near-infrared region by using gold nanorods. J Am Chem Soc 128: 2115–2120.

Huschka R, Barhoumi A, Liu Q, Roth JA, Ji L, Halas NJ (2012). Gene silencing by gold nanoshell-mediated delivery and laser-triggered release of antisense oligonucleotide and siRNA. ACS Nano 6: 7681–7691.

Janib SM, Moses AS, MacKay JA (2010). Imaging and drug delivery using theranostic nanoparticles. Adv Drug Deliv Rev 62: 1052–1063.

Jin Y, Wang J, Ke H, Wang S, Dai Z (2013). Graphene oxide modified PLA microcapsules containing gold nanoparticles for ultrasonic/CT bimodal imaging guided photothermal tumor therapy. Biomaterials 34: 4794–4802.

Kam NWS, O'Connell M, Wisdom J, Dai H (2005). Carbon nanotubes as multifunctional biological transporters and near-infrared agents for selective cancer cell destruction. Proc Natl Acad Sci U S A 102: 11600–11605.

Khandare JJ, Jalota-Badhwar A, Satavalekar SD, Bhansali SG, Aher ND, Kharas F *et al.* (2012). PEG-conjugated highly dispersive multifunctional magnetic multi-walled carbon nanotubes for cellular imaging. Nanoscale 4: 837–844.

Kim C, Song HM, Cai X, Yao J, Wei A, Wang LV (2011). *In vivo* photoacoustic mapping of lymphatic systems with plasmon-resonant nanostars. J Mater Chem 21: 2841–2844.

Kim IT, Nunnery GA, Jacob K, Schwartz J, Liu X, Tannenbaum R (2010). Synthesis, characterization, and alignment of magnetic carbon nanotubes tethered with maghemite nanoparticles. J Phys Chem C 114: 6944–6951.

Kim JW, Galanzha EI, Shashkov EV, Moon HM, Zharov VP (2009). Golden carbon nanotubes as multimodal photoacoustic and photothermal high-contrast molecular agents. Nat Nanotechnol 4: 688–694.

Kim TH, Lee KB, Choi JW (2013). 3D graphene oxide-encapsulated gold nanoparticles to detect neural stem cell differentiation. Biomaterials 34: 8660–8670.

Kostarelos K, Bianco A, Prato M (2009). Promises, facts and challenges for carbon nanotubes in imaging and therapeutics. Nat Nanotechnol 4: 627–633.

Lacerda L, Russier J, Pastorin G, Herrero MA, Venturelli E, Dumortier H *et al.* (2012). Translocation mechanisms of chemically functionalised carbon nanotubes across plasma membranes. Biomaterials 33: 3334–3343.

Lamanna G, Garofalo A, Popa G, Wilhelm C, Bégin-Colin S, Felder-Flesch D *et al.* (2013). Endowing carbon nanotubes with superparamagnetic properties: applications for cell labeling, MRI cell tracking and magnetic manipulations. Nanoscale 5: 4412–4421.

Laurent S, Forge D, Port M, Roch A, Robic C, Vander EL *et al.* (2008). Magnetic iron oxide nanoparticles: synthesis, stabilization, vectorization, physicochemical characterizations, and biological applications. Chem Rev 108: 2064–2110.

Li B, Cao H, Shao J, Qu M (2011). Enhanced anode performances of the Fe_3O_4-carbon-rGO three dimensional composite in lithium ion batteries. Chem Commun 47: 10374–10376.

Li J, Zhu Y, Li W, Zhang X, Peng Y, Huang Q (2010). Nanodiamonds as intracellular transporters of chemotherapeutic drug. Biomaterials 31: 8410–8418.

Li W, Gao C, Qian H, Ren J, Yan D (2006). Multiamino-functionalized carbon nanotubes and their applications in loading quantum dots and magnetic nanoparticles. J Mater Chem 16: 1852–1859.

Lim DK, Barhoumi A, Wylie RG, Reznor G, Langer RS, Kohane DS (2013). Enhanced photothermal effect of plasmonic nanoparticles coated with reduced graphene oxide. Nano Lett 13: 4075–4079.

Link S, El-Sayed MA (2000). Shape and size dependence of radiative, non-radiative and photothermal properties of gold nanocrystals. Int Rev Phys Chem 19: 409–453.

Liu K, Wang Y, Kong X, Liu X, Zhang Y, Tu L *et al.* (2014a). Multispectral upconversion luminescence intensity ratios for ascertaining the tissue imaging depth. Nanoscale 6: 9257–9263.

Liu Q, Wei L, Wang J, Peng F, Luo D, Cui R *et al.* (2012). Cell imaging by graphene oxide based on surface enhanced Raman scattering. Nanoscale 4: 7084–7089.

Liu Y, Jiang W, Li S, Li F (2009). Electrostatic self-assembly of Fe_3O_4 nanoparticles on carbon nanotubes. Appl Surf Sci 255: 7999–8002.

Liu Y, Jiao Y, Qu F, Gong L, Wu X (2013a). Facile synthesis of template-induced SnO_2 nanotubes. J Nanomater 2013: 610964.

Liu Y, Hughes TC, Muir BW, Waddington LJ, Gengenbach TR, Easton CD *et al.* (2014b). Water-dispersible magnetic carbon nanotubes as T2-weighted MRI contrast agents. Biomaterials 35: 378–386.

Liu Z, Liang X-J (2012). Nano-carbons as theranostics. Theranostics 2: 235–237.

Liu Z, Robinson JT, Sun X, Dai H (2008). PEGylated nanographene oxide for delivery of water-insoluble cancer drugs. J Am Chem Soc 130: 10876–10877.

Liu Z, Guo Z, Zhong H, Qin X, Wan M, Yang B (2013b). Graphene oxide based surface-enhanced Raman scattering probes for cancer cell imaging. Phys Chem Chem Phys 15: 2961–2966.

Lu YJ, Wei KC, Ma CC, Yang SY, Chen JP (2012). Dual targeted delivery of doxorubicin to cancer cells using folate-conjugated magnetic multi-walled carbon nanotubes. Colloids Surf B Biointerfaces 89: 1–9.

Ma X, Tao H, Yang K, Feng L, Cheng L, Shi X *et al.* (2012). A functionalized graphene oxide-iron oxide nanocomposite for magnetically targeted drug delivery, photothermal therapy, and magnetic resonance imaging. Nano Res 5: 199–212.

Ma X, Qu Q, Zhao Y, Luo Z, Zhao Y, Ng KW *et al.* (2013). Graphene oxide wrapped gold nanoparticles for intracellular Raman imaging and drug delivery. J. Mater. Chem. B 1: 6495–6500.

Madani SY, Naderi N, Dissanayake O, Tan A, Seifalian AM (2011). A new era of cancer treatment: carbon nanotubes as drug delivery tools. Int J Nanomedicine 6: 2963–2979.

Madani SY, Shabani F, Dwek MV, Seifalian AM (2013). Conjugation of quantum dots on carbon nanotubes for medical diagnosis and treatment. Int J Nanomedicine 8: 941–950.

Masotti A, Caporali A (2013). Preparation of magnetic carbon nanotubes (Mag-CNTs) for biomedical and biotechnological applications. Int J Mol Sci 14: 24619–24642.

Mehdipoor E, Adeli M, Bavadi M, Sasanpour P, Rashidian B (2011). A possible anticancer drug delivery system based on carbon nanotube–dendrimer hybrid nanomaterials. J Mater Chem 21: 15456–15463.

Meng L, Niu L, Li L, Lu Q, Fei Z, Dyson PJ (2012). Gold nanoparticles grown on ionic liquid-functionalized single-walled carbon nanotubes: new materials for photothermal therapy. Chem Eur J 18: 13314–13319.

Meng L, Xia W, Liu L, Niu L, Lu Q (2014). Golden single-walled carbon nanotubes prepared using double layer polysaccharides bridge for photothermal therapy. ACS Appl Mater Interfaces 6: 4989–4996.

Minati L, Antonini V, Dalla Serra M, Speranza G (2012). Multifunctional branched gold–carbon nanotube hybrid for cell imaging and drug delivery. Langmuir 28: 15900–15906.

Narayanan TN, Reena Mary AP, Shaijumon MM, Ci L, Ajayan PM, Anantharaman MR (2009). On the synthesis and magnetic properties of multiwall carbon nanotube-superparamagnetic iron oxide nanoparticle nanocomposites. Nanotechnology 20: 055607.

Nie S, Emory SR (1997). Probing single molecules and single nanoparticles by surface-enhanced Raman scattering. Science 275: 1102–1106.

Pan Y, Bao H, Sahoo NG, Wu T, Li L (2011). Water-soluble poly(N-isopropylacrylamide)-graphene sheets synthesized via click chemistry for drug delivery. Adv Funct Mater 21: 2754–2763.

Pawson AJ, Sharman JL, Benson HE, Faccenda E, Alexander SP, Buneman OP *et al.*; NC-IUPHAR (2014). The IUPHAR/BPS Guide to PHARMACOLOGY: an expert-driven knowledgebase of drug targets and their ligands. Nucl. Acids Res. 42 (Database Issue): D1098–106.

Qian X, Peng XH, Ansari DO, Yin-Goen Q, Chen GZ, Shin DM *et al.* (2008a). *In vivo* tumor targeting and spectroscopic detection with surface-enhanced Raman nanoparticle tags. Nat Biotech 26: 83–90.

Qian XM, Nie SM (2008b). Single-molecule and single-nanoparticle SERS: from fundamental mechanisms to biomedical applications. Chem Soc Rev 37: 912–920.

Robinson JT, Tabakman SM, Liang Y, Wang H, Sanchez Casalongue H, Vinh D *et al.* (2011). Ultrasmall reduced graphene oxide with high near-infrared absorbance for photothermal therapy. J Am Chem Soc 133: 6825–6831.

Sajja HK, East MP, Mao H, Wang AY, Nie S, Yang L (2009). Development of multifunctional nanoparticles for targeted drug delivery and non-invasive imaging of therapeutic effect. Curr Drug Discov Technol 6: 43–51.

Schöppler F, Mann C, Hain TC, Neubauer FM, Privitera G, Bonaccorso F *et al.* (2011). Molar extinction coefficient of single-wall carbon nanotubes. J Phys Chem C 115: 14682–14686.

Shen X, Wu J, Bai S, Zhou H (2010). One-pot solvothermal syntheses and magnetic properties of graphene-based magnetic nanocomposites. J Alloys Compd 506: 136–140.

Shi X, Gong H, Li Y, Wang C, Cheng L, Liu Z (2013). Graphene-based magnetic plasmonic nanocomposite for dual bioimaging and photothermal therapy. Biomaterials 34: 4786–4793.

Shibu ES, Hamada M, Murase N, Biju V (2013). Nanomaterials formulations for photothermal and photodynamic therapy of cancer. J Photochem Photobiol C Photochem Rev 15: 53–72.

Singh R, Torti SV (2013). Carbon nanotubes in hyperthermia therapy. Adv Drug Deliv Rev 65: 2045–2060.

Smith AH, Robinson EM, Zhang XQ, Chow EK, Lin Y, Osawa E *et al.* (2011). Triggered release of therapeutic antibodies from nanodiamond complexes. Nanoscale 3: 2844–2848.

Tung LD, Kolesnichenko V, Caruntu D, Chou NH, O'Connor CJ, Spinu L (2003). Magnetic properties of ultrafine cobalt ferrite particles. J Appl Phys 93: 7486–7488.

Turcheniuk K, Khanal M, Motorina A, Subramanian P, Barras A, Zaitsev V *et al.* (2014). Insulin loaded iron magnetic nanoparticle–graphene oxide composites: synthesis, characterization and application for *in vivo* delivery of insulin. RSC Adv 4: 865–875.

Villalonga R, Villalonga ML, Díez P, Pingarrón JM (2011). Decorating carbon nanotubes with polyethylene glycol-coated magnetic nanoparticles for implementing highly sensitive enzyme biosensors. J Mater Chem 21: 12858–12864.

Wang C, Li J, Amatore C, Chen Y, Jiang H, Wang XM (2011). Gold nanoclusters and graphene nanocomposites for drug delivery and imaging of cancer cells. Angew Chem Int Ed 50: 11644–11648.

Wang C, Ravi S, Garapati US, Das M, Howell M, Mallela J *et al.* (2013a). Multifunctional chitosan magnetic-graphene (CMG) nanoparticles: a theranostic platform for tumor-targeted co-delivery of drugs, genes and MRI contrast agents. J Mater Chem B 1: 4396–4405.

Wang H, Wang Z, Ye M, Zong S, Li M, Chen P *et al.* (2014a). Optically encoded nanoprobes using single walled carbon nanotube as the building scaffold for magnetic field guided cell imaging. Talanta 119: 144–150.

Wang X, Wang C, Cheng L, Lee ST, Liu Z (2012). Noble metal coated single-walled carbon nanotubes for applications in surface enhanced Raman scattering imaging and photothermal therapy. J Am Chem Soc 134: 7414–7422.

Wang Y, Wang H, Liu D, Song S, Wang X, Zhang H (2013b). Graphene oxide covalently grafted upconversion nanoparticles for

combined NIR mediated imaging and photothermal/photodynamic cancer therapy. Biomaterials 34: 7715–7724.

Wang Y, Wang K, Zhao J, Liu X, Bu J, Yan X *et al.* (2013c). Multifunctional mesoporous silica-coated graphene nanosheet used for chemo-photothermal synergistic targeted therapy of glioma. J Am Chem Soc 135: 4799–4804.

Wang Y, Huang R, Liang G, Zhang Z, Zhang P, Yu S *et al.* (2014b). MRI-visualized, dual-targeting, combined tumor therapy using magnetic graphene-based mesoporous silica. Small 10: 109–116.

Webb JA, Bardhan R (2014). Emerging advances in nanomedicine with engineered gold nanostructures. Nanoscale 6: 2502–2530.

Wildgoose GG, Banks CE, Compton RG (2006). Metal nanoparticles and related materials supported on carbon nanotubes: methods and applications. Small 2: 182–193.

Wu H, Liu G, Wang X, Zhang J, Chen Y, Shi J *et al.* (2011). Solvothermal synthesis of cobalt ferrite nanoparticles loaded on multiwalled carbon nanotubes for magnetic resonance imaging and drug delivery. Acta Biomater 7: 3496–3504.

Xu C, Yang D, Mei L, Li Q, Zhu H, Wang T (2013a). Targeting chemophotothermal therapy of hepatoma by gold nanorods/graphene oxide core/shell nanocomposites. ACS Appl Mater Interfaces 5: 12911–12920.

Xu C, Yang D, Mei L, Lu B, Chen L, Li Q *et al.* (2013b). Encapsulating gold nanoparticles or nanorods in graphene oxide shells as a novel gene vector. ACS Appl Mater Interfaces 5: 2715–2724.

Xu P, Cui D, Pan B, Gao F, He R, Li Q *et al.* (2008). A facile strategy for covalent binding of nanoparticles onto carbon nanotubes. Appl Surf Sci 254: 5236–5240.

Xue Y, Chen H, Yu D, Wang S, Yardeni M, Dai Q *et al.* (2011). Oxidizing metal ions with graphene oxide: the in situ formation of magnetic nanoparticles on self-reduced graphene sheets for multifunctional applications. Chem Commun (Camb) 47: 11689–11691.

Yang K, Hu L, Ma X, Ye S, Cheng L, Shi X *et al.* (2012). Multimodal imaging guided photothermal therapy using functionalized graphene nanosheets anchored with magnetic nanoparticles. Adv Mater 24: 1868–1872.

Yang X, Zhang X, Ma Y, Huang Y, Wang Y, Chen Y (2009). Superparamagnetic graphene oxide–Fe_3O_4 nanoparticles hybrid for controlled targeted drug carriers. J Mater Chem 19: 2710–2714.

Yang X, Wang Y, Huang X, Ma Y, Huang Y, Yang R *et al.* (2011). Multi-functionalized graphene oxide based anticancer drug-carrier with dual-targeting function and pH-sensitivity. J Mater Chem 21: 3448–3454.

Yavuz MS, Cheng Y, Chen J, Cobley CM, Zhang Q, Rycenga M *et al.* (2009). Gold nanocages covered by smart polymers for controlled release with near-infrared light. Nat Mater 8: 935–939.

Yin M, Wang M, Miao F, Ji Y, Tian Z, Shen H *et al.* (2012). Water-dispersible multiwalled carbon nanotube/iron oxide hybrids as contrast agents for cellular magnetic resonance imaging. Carbon 50: 2162–2170.

Zavaleta C, de la Zerda A, Liu Z, Keren S, Cheng Z, Schipper M *et al.* (2008). Noninvasive Raman spectroscopy in living mice for evaluation of tumor targeting with carbon nanotubes. Nano Lett 8: 2800–2805.

Zhang W, Guo Z, Huang D, Liu Z, Guo X, Zhong H (2011). Synergistic effect of chemo-photothermal therapy using PEGylated graphene oxide. Biomaterials 32: 8555–8561.

Zhang X, Li Y, Cao C (2012). Facile one-pot synthesis of mesoporous hierarchically structured silica/carbon nanomaterials. J Mater Chem 22: 13918–13921.

Zhang XQ, Chen M, Lam R, Xu X, Osawa E, Ho D (2009). Polymer-functionalized nanodiamond platforms as vehicles for gene delivery. ACS Nano 3: 2609–2616.

Zhou H, Zhang C, Li H, Du Z (2010). Decoration of Fe_3O_4 nanoparticles on the surface of poly (acrylic acid) functionalized multi-walled carbon nanotubes by covalent bonding. J Polym Sci Part A Polym Chem 48: 4697–4703.